Author/s:
Datta, S;Karmakar, CK;Rao, AS;Yan, B;Palaniswami, M

Title:
Upper limb movement profiles during spontaneous motion in acute stroke

Date:
2021-05-11

Citation:
Datta, S., Karmakar, C. K., Rao, A. S., Yan, B. & Palaniswami, M. (2021). Upper limb movement profiles during spontaneous motion in acute stroke. Physiological Measurement, 42 (4), https://doi.org/10.1088/1361-6579/abf01e.

Persistent Link:
https://hdl.handle.net/11343/302063

Upper limb movement profiles during spontaneous motion in acute stroke

Shreyasi Datta[1], Chandan K. Karmakar[2], Aravinda S. Rao[1], Bernard Yan[3], Marimuthu Palaniswami[1]

[1] Department of Electrical and Electronic Engineering, University of Melbourne
[2] School of Information Technology, Deakin University
[3] Department of Neurology, Royal Melbourne Hospital

E-mail: shreyasid@student.unimelb.edu.au

Abstract. Objective: Clinical assessment of upper limb hemiparesis in acute stroke involves repeated manual examination of hand movements during instructed tasks. This process is labour-intensive and prone to human errors while also being strenuous for the patient. Wearable motion sensors can automate the process by measuring characteristics of hand activity. Existing work in this direction either use multiple sensors or complex instructed movements, or analyze only the *quantity* of upper limb motion. These methods are obtrusive and strenuous for acute stroke patients and also sensitive to noise. In this work, we propose to use only two wrist-worn accelerometer sensors to study the *quality* of completely spontaneous upper limb motion and investigate correlation with clinical scores for acute stroke care. Approach: Velocity time series estimated from acquired acceleration data during spontaneous motion is decomposed into smaller movement elements. Measures of density, duration and smoothness of these component elements are extracted and their disparity is studied across the two hands. Main results: Spontaneous upper limb motion in acute stroke can be decomposed into movement elements that resemble point-to-point reaching tasks. These elements are smoother and sparser in the normal hand than the hemiparetic hand, and the amount of smoothness correlates with hemiparetic severity. Features characterizing the disparity of these movement elements between two hands show statistical significance in differentiating mild-to-moderate and severe hemiparesis. Using data from 67 acute stroke patients, the proposed method can classify the two levels of hemiparetic severity with 85% accuracy. Additionally, compared to activity based features, the proposed method is robust to the presence of noise in acquired data. Significance: This work demonstrates that the quality of upper limb motion can characterize and identify hemiparesis in stroke survivors. This is clinically significant towards continuous automated assessment of hemiparesis in acute stroke using minimally intrusive wearable sensors.

Keywords: Accelerometry, hemiparesis, point-to-point movement, stroke, upper limb weakness, velocity profile, wearable sensors.

1. Introduction

Stroke is a leading cause of global concern, accounting for 5.5 million deaths and the loss of several million years of healthy life from related disabilities every year [1,2]. The World Health Organization (WHO) reports that one in four people above 25 years of age is likely to suffer a stroke [2]. Lack of signal transmission from the motor cortex, responsible for generating movement impulses, leads to motor impairments and paralysis, within 24 hours of stroke onset [3, 4]. Paralysis in one half of the body or *hemiparesis*, affects the upper limbs by limiting movements and co-ordination [5]. During the *acute* phase, *i.e.*, while in medical care after the attack, the severity of hemiparesis is monitored at regular intervals to assess the efficacy of *reperfusion* therapy for restoring blood flow and to prevent recurrent strokes [5, 6]. The clinical gold standard for such assessment is the National Institutes of Health Stroke Scale (NIHSS), assigned by studying the strength of a patient's hands held against gravity [7]. This process needs to be carried out repeatedly at regular intervals throughout the day, thereby requiring 24x7 supervision by trained medical personnel. Therefore, the process is labour-intensive, prone to human errors and inter-rater variability, and at the same time, stressful and exhausting for the patient [5].

Wearable devices with motion sensors are effective in automated identification of neurological disorders including strokes [6, 8]. Wearable accelerometry can be used to quantify the amount of upper limb use in post-stroke hemiparetic patients based on *activity count* [9]. Various time and frequency domain features from accelerometer data correlate well with clinical scores in stroke patients [10–14]. Most of such literature focus on activity monitoring during rehabilitation, after patients are discharged from the hospital. Usually several sensors are attached to different parts of the body and subjects have to perform complex instructed tasks for data acquisition. Such methods are not suitable for assessing hemiparesis progression in acute stroke patients in the hospital environment, because of discomfort and burden associated with multiple sensors and complex tasks. In our previous works [6, 15], we used only two wrist-worn accelerometers to quantify relative activity between two hands in acute stroke patients and proposed measures that correlate with NIHSS. In more recent works, we showed that characteristics of spontaneous and instructed activities in acute stroke patients can be used to predict NIHSS scores using short-length data from wrist-worn accelerometers [5, 16, 17]. These methods are based on quantifying the similarity between the activity patterns between two hands using measures of *correlation* or *distance*. They measure the *quantity* of relative motion, *i.e.*, to what extent and how frequently the hemiparetic hand is used compared to the normal hand. However, these methods fail to consider the *quality* of hand movements, *i.e.*, the nature or patterns in the motion which relate to motor functionality in terms of muscle and joint biomechanics [18, 19]. Additionally, these include instructed activities to study motion characteristics, instead of naturally occurring spontaneous motion that is more clinically significant in monitoring acute and sub-acute stroke patients.

Qualitative analysis of upper limb motion in stroke patients during rehabilitation relate to optimization of movements by the central nervous system [19]. In a recent work [20], correlation between movement quality and functional ability was investigated in rehabilitative patients using sensors on the sternum and wrist during a minimally burdensome motor task. Motivated by this, in this paper, we investigate the quality of relative motion between two hands in acute stroke patients during *completely* spontaneous activities without any task instructions, and only two wrist-worn accelerometers. We base our analysis on the seminal model for point-to-point upper limb movements based on the minimum *jerk* principle [21,22] and investigate novel features that characterize such motion in stroke patients. This work is a continuation of our research on wearable based acute stroke monitoring [5, 6, 23] to (i) estimate the characteristics of *component* movement elements of hemiparetic hands during spontaneous motion, (ii) study their deviations from those of healthy hand movements and (iii) find measures of qualitative relative motion between two hands that might correlate with hemiparetic severity. We show that spontaneous upper limb motion can be decomposed into point-to-point reaching tasks with velocity profiles similar to that found in healthy individuals, and additionally, features derived from those profiles describe the relative motion between two hands and correlate with hemiparesis severity. This is particularly relevant in a hospital scenario as the data includes only spontaneous activities and is acquired in a minimally intrusive way using two wristwatch-like wearable sensors.

2. Background

A mathematical model of voluntary upper limb motion based on behavioural organization in primates was introduced in [21]. The model focused on the goal of making the smoothest possible movement under the given circumstances, *i.e.*, by minimizing *accelerative transients*. This was formalized by using dynamic optimization to minimize an objective function that estimates the rate of change of acceleration or *jerk* during the movement. This minimum jerk hypothesis to describe pointing movements towards a target yield symmetric, bell-shaped velocity profiles, if the target has zero velocity and acceleration at the start and end of movement. This study was extended in [22] to investigate unconstrained hand motion between two points in the horizontal plane. It was found that the trajectory yielded symmetric bell-shaped velocity profiles as predicted before and the path was approximately a straight line. The minimum jerk objective function was further extended by Hoff [24] to include a penalty for movement duration in point-to-point reaching movements. This model considers the quickness and the effort in making smooth motion between two points and provides the optimal movement duration along with the optimal trajectory. For two dimensional hand movement, such an objective function can be written as (1).

$$I = t_f + K \int_{t=0}^{t=t_f} (u_x^2 + u_y^2) dt \tag{1}$$

Here, u_x and u_y are the time series representing jerk along X and Y axes respectively, and the movement starts and ends at times $t = 0$ and $t = t_f$ respectively. K is a positive constant, weighting between the *time* and *jerk* components in the objective function. Assuming static boundary conditions, it can be shown that the position trajectories are straight lines between the two points and a fifth-order polynomial in time as in (2) for $i \in \{x, y\}$ [21,22], which leads to the bell-shaped velocity profile obeying (3) [24].

$$p_i(t) = D\left[6\left(t/t_f\right)^5 - 15\left(t/t_f\right)^4 + 10\left(t/t_f\right)^3\right] \tag{2}$$

$$v_i(t) = D\left[30\left(t^4/t_f^5\right) - 60\left(t^3/t_f^4\right) + 30\left(t^2/t_f^3\right)\right] \tag{3}$$

Here D denotes the associated displacement. The relationship between the movement duration t_f and displacement is given by (4).

$$t_f = (60D)^{1/3}K^{1/6} \tag{4}$$

It is important to note that this framework was developed for two-dimensional point-to-point reaching movements. In a recent work, Miranda *et al.* found that complex upper limb motion such as drawing and writing on 2D planes as well as 3D movements can be modeled as combinations of primitive movement components in a Cartesian coordinate system with axes oriented in the medio-lateral, antero-posterior and vertical directions [25]. These primitive components actually resemble 1D point-to-point reaching movements, resulting in bell-shaped velocity profiles. This study suggests that complex upper limb motion actually comprises a series of point-to-point reaching tasks with intermediate targets that show similar characteristics with those for reaching tasks studied in [24]. This work has been extended to investigate the quality of upper limb motion in stroke survivors during rehabilitation from wearable accelerometer data [19,20]. Such methodology is dependent on acquiring reference motion data from a waist-worn sensor (for transforming the upper limb motion into anatomical frames) [20] or reference velocity profiles from healthy controls (to segregate the acceleration data into meaningful groups) [19].

In this work, we analyze upper limb velocity profiles by decomposing spontaneous motion to component point-to-point movements using only wrist-worn accelerometers, without any reference sensor or data. We find that the *disparity* between the movement profiles in two hands convey important information regarding hemiparetic severity in acute stroke patients. We show that features measuring this disparity can be used to classify *mild-to-moderate* and *severe* hemiparesis even with noisy data. Therefore, this work is a preliminary step towards a wearable based automated hemiparesis progression monitoring system based on upper-limb motion quality analysis in acute stroke patients.

3. Methods

3.1. Data Acquisition

NIHSS for quantifying motor weakness in acute stroke is a 5-point scale that encodes the strength of an upper limb against gravity, with 0 indicating normal strength and 4

indicating no movements or a completely dead arm [5]. Manual NIHSS administration requires careful observation of the duration and drift from the horizontal while hands are held up against the gravity. Though wrist-worn accelerometers can capture these movements, unless accurate time-stamps for each movement phase (*i.e.*, lifting, holding, dropping of hands) are available, such data is not reliable [5]. Additionally, repeating such an exercise multiple times throughout the day is strenuous for acute stroke patients. Therefore, in this paper, we study completely spontaneous motion performed by patients for short durations. We investigate such motion for two fundamental levels of hemiparetic severity, *i.e.*, *mild-to-moderate* (comprising NIHSS 1 and 2) and *severe* (comprising NIHSS 3 and 4). This is based on the fact that subjects in NIHSS 3 and 4 cannot lift their hands and those in NIHSS 1 and 2 can lift them for lesser durations than a healthy person [5].

Patients were recruited at the stroke units of the Royal Melbourne Hospital, Australia and Sree Chitra Tirunal Institute for Medical Sciences and Technology, India with their informed consents. The data acquisition protocol was approved by the respective institute's human research ethics committee (RMH HREC 2016.146 and SCT/IEC/1081/October-2017). The screening criteria for patient recruitment was the presence of an upper limb weakness due to an ischemic stroke within the past 5 days of data acquisition. The diagnosis of stroke was verified clinically by an expert neurologist through neuroimaging [5]. Data acquisition protocol involves (i) NIHSS scoring (subject is asked to lift up and hold arms horizontally for 10 seconds during which the clinical hemiparesis score for each arm is determined by a nurse and (ii) spontaneous movements (subject is encouraged to move their hands as much as possible in the vertical and horizontal directions and perform simple tasks *e.g.*, lifting a cup, moving a pen and using a phone). The average data length across all subjects was 3.32±1.33 minutes.

Table 1: Description of acquired data

Hemiparesis Severity	Clinical Description	Subjects	Left Affected	Females	Age
Mild-to-Moderate (NIHSS 1 - 2)	Can lift up hands and hold against gravity for <=10 secs, with drifts from horizontal	35	19	11	63.9±13.9
Severe (NIHSS 3 - 4)	Cannot lift up hands, may perform minor movements at the wrist	32	16	12	64.4±14.5

Overall, data was acquired from 67 patients (34.33% female, 64.15±14.08 years old) who had a stroke in the past 5±4 days resulting in a weak arm with mild-to-moderate (NIHSS 1 or 2) or severe (NIHSS 3 or 4) hemiparesis as detailed in Table 1. More than 80% of the recruited patients were characterized by Total/Partial Anterior Circulation Infarcts (TACI/PACI) [26] and a history of hypertension. For each level of hemiparesis, the affected arm was assigned a score presented in the column labeled NIHSS, whereas,

the other arm was labeled as normal, *i.e.*, NIHSS 0. Data was collected using two low-cost wearable wrist-worn sensors with triaxial accelerometers from Eoxys [5]. The accelerometers acquired data at a sampling rate of 100 Hz and with a full scale range of $\pm 8g$. The sensors communicate via bluetooth to a smartphone application that records data continuously and sends over to a remote server for storage.

3.2. Estimation and Analysis of Movement Profiles

In this work, we have decomposed the spontaneous motion in each hand into component movement profiles, representing point-to-point reaching movements. Then we have analyzed these individual profiles and correlated them with hemiparetic severity. The steps followed in this process are illustrated in Fig. 1 and elaborated below.

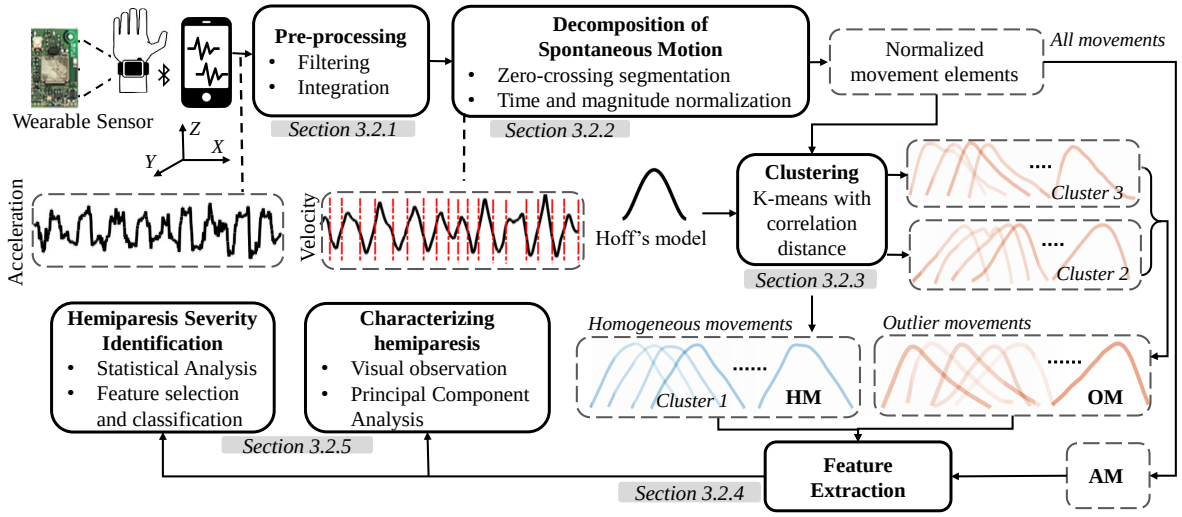

Figure 1: Steps for extracting and processing one-dimensional movement elements from each axis of wrist-worn accelerometer time series to characterize and identify hemiparesis. The pipeline is executed for data acquired from each hand and the disparity of the extracted features between two hands from homogeneous (HM), outlier (OM) and all (AM) movement elements correlate motion quality with hemiparetic severity.

3.2.1. Pre-processing: From the raw accelerometer data, gravitational components of acceleration and high frequency noise are eliminated using a 6^{th} order Butterworth bandpass filter between 0.25 Hz and 8 Hz [27]. Further, a median filter with window length of 3 samples is used to smooth the data [27]. The filtered acceleration data from each axis is trapezoid integrated to obtain a time-series representing *velocity*. This time-series is then filtered using a 6^{th} order Butterworth bandpass filter with cut-off frequencies of 0.1 Hz and 6 Hz to minimize low frequency integration drifts and high frequency noise [20].

3.2.2. Decomposition of Spontaneous Motion: As stated before, it has been shown that 1D movement elements with zero initial and terminal velocities, exhibit a similar,

approximately bell-shaped structure in healthy individuals, that represent the quality of smooth point-to-point motion [20, 24]. Therefore, in order to analyze the quality of motion in acute stroke patients, each session of spontaneous motion along the X, Y and Z axes is decomposed into smaller movement components. This is done by segmenting each velocity time-series at its *zero-crossings*. Movement elements whose duration exceed or is below the mean movement duration by one standard deviation (along each axis and each session), are eliminated from further analysis. The segmented *velocity profiles* are then normalized in time and magnitude for further processing [20]. For time-normalization, each profile is resampled to 100 samples (which is around the mean duration of the movement elements in our dataset). Each profile is then magnitude normalized in [0,1] by normalizing with the maximum velocity in that segment. These methods for normalization retain the morphological characteristics of the velocity profiles of each segment, while making it convenient to compare them between sessions and subjects.

3.2.3. Clustering Velocity Profiles: Time and magnitude normalized velocity profiles for point-to-point motion in healthy individuals can be clustered optimally in three groups as shown in [19]. Here, squared Euclidean distance based k-means clustering was used and Davies-Bouldin index was used to determine the optimal number of clusters. The velocity profiles for stroke survivors were found to follow similar patterns to one of the clusters, and were assigned to them based on their distance from the cluster centroid. Clustering is necessary to identify movements which resemble the actual bell shaped pattern and evaluate their characteristics in stroke patients. In this work, instead of using reference clusters from additional data (acquired from a clinically healthy population), we use Hoff's model as a reference to segregate the velocity profiles for further analysis. Here, first k-means clustering with $k = 3$ is performed using *correlation* as a dissimilarity measure [28]. Correlation based distance in [0,1] is a standard technique to estimate *shape* similarity in magnitude normalized time-series data [29]. The mean time-series representing each cluster is then compared with the bell-shaped Hoff model using correlation as the similarity measure. The cluster with the closest mean based on this similarity is identified to be the cluster of *homogeneous movements* (HM) and the remaining two clusters are identified as *outlier movements* (OM). This naming convention follows [20], though, authors there use *density* based clustering of the velocity profiles, based on the assumption that stroke survivors generate a dense set of homogeneous movement profiles that resemble bell-shaped characteristics. However, as this assumption may or may not be true for completely spontaneous motion in acute stroke, we analyze the clusters based on the deviation from the standard Hoff's model. The set of *all* movement elements comprising HM and OM are referred to as AM hereafter.

3.2.4. Feature Extraction: For each cluster, a set of features are extracted from the velocity profiles along each axis for each hand as tabulated in Table 2. The first set of features include characteristics such as the number (N) and duration (D) of movement

elements. The duration of the element is considered before time-normalization. The next set of features, namely, Euclidean distance ED, Dynamic Time Warping based distance DTW [28] and Cross-Sample Entropy $CrossEn$ [30] represent different forms of similarity or distance of each element to the arithmetic average of the set of movement elements. Finally, the remaining features estimate the shape and smoothness of the velocity profiles through statistical measures or measures of randomness. These include variance, skewness, kurtosis, standard deviation of differences [31], Coefficient of Variation [32], Sample Entropy [33] and Shannon Entropy [5], Hjorth parameters [34] and Poincaré descriptors [31, 35]. Therefore, a total of 20 features are extracted, characterising the velocity profiles of the movement elements. For each feature F^i_j, $i \in \{1, 20\}$ and $j \in \{left, right\}$, the normalized absolute difference of the values between the two hands *i.e.*, $\frac{|F^i_{left} - F^i_{right}|}{F^i_{left} + F^i_{right}}$ is considered for further analysis. This difference encodes the quality of relative motion between the two hands and is hypothesized to be higher for increasing severity of hemiparesis [5].

3.2.5. Correspondence with Hemiparesis: Initially, the visual differences between the characteristics of the movement elements of the normal and hemiparetic hands are studied to support our hypothesis that the movement elements are expected to be different in the two hands. This is supported by Principal Component Analysis [20] to study the density and spread of the velocity profiles of each hand. To determine the correspondence of the quality of spontaneous motion with the severity of hemiparesis in acute stroke patients, the statistical significance of the extracted features is determined by the non-parametric Kruskal-Wallis test across each level of hemiparesis (mild-to-moderate or severe) [5]. To further analyze feature significance for differentiating between the two classes, the Area under the Receiver Operating Characteristics (ROC) curve (AUC) is also studied [16]. Finally, we have used Support Vector Machines (SVMs) with different types of kernel functions [36] to classify the feature space into two classes of hemiparesis. Prior to classification, the minimal-redundancy-maximal-relevance (MRMR) [37] algorithm is employed to select the salient features from all features extracted from HM, OM and AM and create a feature vector corresponding to the data from each subject. This method finds the features which have highest relevance to the target classes while reducing redundancy among the selected features. We have trained the classifier model using 10-fold cross-validation. The overall *Accuracy*, *Sensitivity* (of each class) and *F-score* [36] are reported across all folds of cross-validation.

4. Results

In this section, we present characteristics of the velocity profiles and statistical significance of the proposed features, and also discuss their suitability in hemiparesis identification. All computations are performed using MATLAB R2019b [38].

Table 2: List of features extracted from velocity profiles of movement elements*

Feature	Formulation
Number of elements (N)	Total number of movement elements in a session
Element duration (D)	Time duration of a movement element prior to time normalization
Euclidean distance (ED)#	$\sqrt{\sum_i (x_i - x_i^{avg})^2}$
Dynamic Time Warping distance (DTW)#	$min(\sum_{i=1}^{s} w_i)$
Cross-Sample Entropy ($CrossEn$)#ˆ	$\ln \frac{\phi^m(r)}{\phi^{m+1}(r)}$, $\phi^m(r) = \frac{1}{n-m} \sum_{i=1}^{n-m} X_i^m(r)$
Variance (Var)	$\frac{\sum_i (x_i - \overline{x})^2}{n}$
Standard deviation of successive differences ($SDSD$)	$\sqrt{\frac{\sum_i (x'_i - \overline{x'})^2}{n}}$
Coefficient of Variation (CV)	$\frac{\sqrt{\frac{\sum_i (x_i - \overline{x})^2}{n}}}{\overline{x}}$
Coefficient of Variation of differences (dCV)	$\frac{\sqrt{\frac{\sum_i (x'_i - \overline{x'})^2}{n-1}}}{\overline{x'}}$
Sample Entropy ($SampEn$)ˆ	$\ln \frac{\phi^m(r)}{\phi^{m+1}(r)}$, $\phi^m(r) = \frac{1}{n-m} \sum_{i=1}^{n-m} C_i^m(r)$
Shannon Entropy ($ShannEn$)	$-\sum_i x_i^2 \log(x_i^2)$
Skewness (Sk)	$E[(\frac{x-\overline{x}}{\sigma})^3]$
Kurtosis ($Kurt$)	$E[(\frac{x-\overline{x}}{\sigma})^4]$
Hjorth Mobility (Mob)	$\sqrt{\frac{Var(x')}{Var(x)}}$
Hjorth Complexity ($Comp$)	$\frac{Mob(x')}{Mob(x)}$
Teager Energy (TE)	$\sqrt{\frac{1}{N} \sum_{i=3}^{n} (x_{i-1}^2 - x_i x_{i-2})}$
$SD1$+	$\sqrt{\frac{1}{2} SDSD^2}$
$SD2$+	$\sqrt{2\sigma^2 - \frac{1}{2} SDSD^2}$
Complex Correlation Measure (CCM)+	$\frac{1}{\pi \times SD1 \times SD2} \sum_{i=1}^{n-3} \lvert A_i \rvert$
SD Ratio (SDR) +	$SD1/SD2$

* Extracted on movement element time series x. Sum of distance based features ED, DTW and $CrossEn$ and median of all other features except N taken over all movement elements. x', $\overline{x}$, σ and n denote successive differences series, mean, standard deviation and length of x.
# Distance features compute the similarity of each element x with the average element x^{avg} of that set. For DTW, $[w_1, ..., w_s], s >= n$ is a warping path representing mapping between x and x^{avg} [28].
ˆSample entropy based features, where $C_i^m(r)$ and $X_i^m(r)$ denote the probabilities of a pattern of length m in x to lie within distance r of another pattern in x or a pattern in x^{avg}, $m = 2$ and $r = 0.15 \times \sigma$ [30,33].
+ Poincare descriptors, $|A_i|$ in CCM denotes the the area of a triangle comprised of three consecutive pairs of points (x_i, x_{i+1}), (x_{i+1}, x_{i+2}) and (x_{i+2}, x_{i+3}) [35]

4.1. Nature of Velocity Profiles

Fig. 2 shows the time and magnitude normalized velocity profiles for HM and OM (in dotted coloured lines) and their means (in solid black line) for two representative subjects, one with mild-to-moderate hemiparesis in the left hand (Figs. 2(a) - 2(d)) and the other with severe hemiparesis in the right hand (Figs. 2(e) - 2(h)). In both cases, the homogeneous movements follow approximately bell-shaped velocity profiles, closely resembling Hoff's model, across all sensor axes. The outlier movements, on the

other hand, are more chaotic and spread out than the dense and compact homogenenous movement elements. OM, in effect, comprises two sets of movement elements (following Section 3.2.3), one that reach peak velocity earlier (cluster 3 in Fig. 1), and another that reach peak velocity later (cluster 2 in Fig. 1) than the bell shaped profiles that reach the peak velocity approximately in the middle. For HM, the normal hands (Figs. 2(b) and 2(e)) exhibit smoother profiles than the affected hands (Figs. 2(a) and 2(f)) for both classes of hemiparesis, though the disparity between the two hands appear more prominent in severe hemiparesis. For OM, there is not much visible difference between the two hands in mild-to-moderate hemiparesis (Figs. 2(c) and 2(d)). However, for severe hemiparesis the affected hand (Fig. 2(h)) has distinctly larger density and spread of movement elements than the normal hand (Fig. 2(g)).

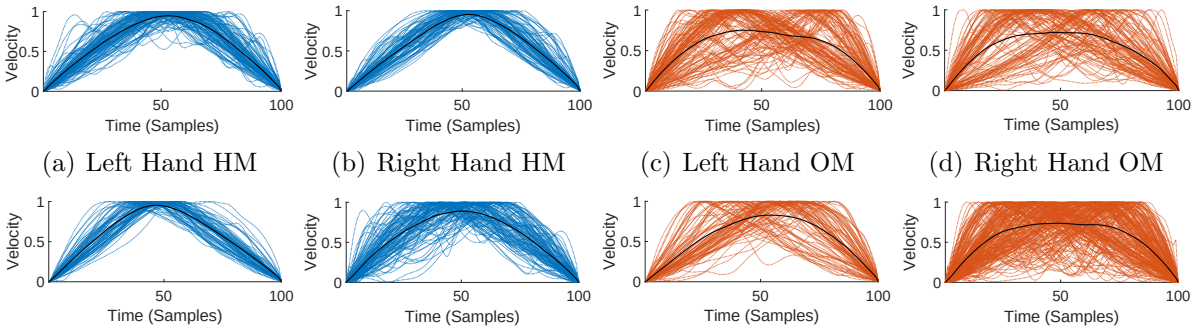

(a) Left Hand HM (b) Right Hand HM (c) Left Hand OM (d) Right Hand OM

(e) Left Hand HM (f) Right Hand HM (g) Left Hand OM (h) Right Hand OM

Figure 2: Time and magnitude normalized velocity profiles of both types of movement elements *i.e.*, HM (—) and OM (—) accumulated along all three axes with their means (—), from two subjects: top row (a)-(d) with mild hemiparesis (NIHSS 1) in the left hand and bottom row (e)-(h) with severe hemiparesis (NIHSS 4) in the right hand.

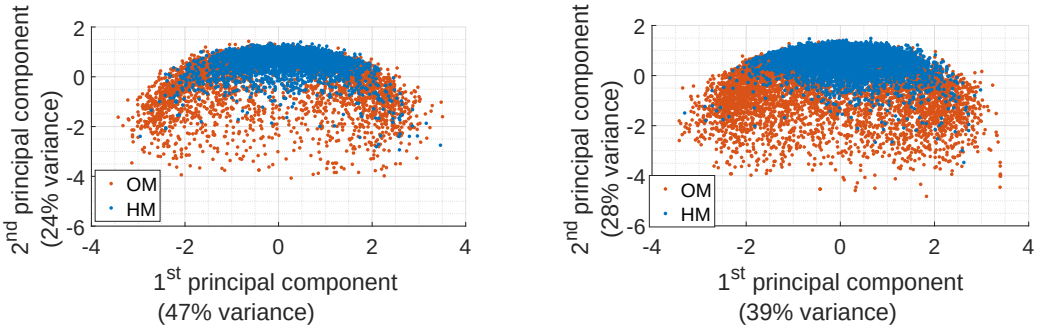

(a) Normal Hand (b) Hemiparetic Hand

Figure 3: 2D projection of the first two principal components obtained using PCA on time and magnitude normalized velocity profiles of the homogeneous and outlier movement elements obtained from all subjects with severe hemiparesis.

To further investigate the disparity in the movement elements of the two hands in severe hemiparesis, we perform Principal Component Analysis (PCA) of the time

series representing the velocity profiles [20]. 2D projections of these movement elements showing the first two principal components, that account for 71% and 67% of the total variance in the normal and affected hands respectively, are illustrated in Fig. 3. As observed earlier, HM comprise a dense and more compact region among all movement elements for both the hands. However, for both types of movements, the elements in the normal hand appear sparse, while that in the affected hand are denser and more spread out. HM contained 49% and 45.82% of all normalized movement elements for mild-to-moderate and severe hemiparetic subjects respectively. This indicates that though acute stroke patients exhibit the well known bell-shaped morphology (constituting HM) in velocity profiles during spontaneous motion, a significant amount (over 50%) of the movement elements deviate from this pattern (constituting OM).

4.2. Statistical Analysis of Features

Next, we present a statistical analysis of the features derived from the velocity profiles of the movement elements in identifying the severity of hemiparesis. This is illustrated through the AUC obtained from ROC curves and the p-value of the Kruskal Wallis test in Table 3, separately for HM, OM and AM. All features except CV, Sk and $Kurt$ are statistically significant with $p < 0.01$ and AUCs above 0.70 for any type of movement. Furthermore, the features D, N, ED, DTW, $CrossEn$, $SDSD$, $ShannEn$, Mob, $Comp$, TE and $SD1$ are statistically (highly) significant with $p < 0.001$ across all types of movements. The top features with AUCs>0.85 include D across all types movements, and N and $CrossEn$ for AM. Overall, it is observed that AM produces higher AUCs than HM or OM individually, for most of the features. Fig. 4 shows the *box plots* of the distribution of these features across the two classes of hemiparesis for AM (HM and OM follow similar patterns and observations from Table 3). The feature values representing the normalized difference of the feature across the affected and the normal hand, tend to have higher median value and larger variance in severe hemiparesis. All features except Sk and $Kurt$ have considerable difference among the median values of the two classes. Following Table 3, for all movement elements comprising AM, the statistically (highly) significant features ($p < 0.001$) D, N, ED, DTW, $CrossEn$, Var, $SDSD$, dCV, $ShannEn$, Mob, $Comp$, TE, $SD1$ and SDR show no overlap in the interquartile ranges (boxes) between mild-to-moderate and severe hemiparesis.

The suitability of the velocity profile based features, for identifying hemiparetic severity in acute stroke from spontaneous movements can be visually observed from 3D scatter plots of the top features. These are illustrated in Fig. 5 for each type of movement. The top three features are chosen based on the AUC values in Table 3. Each of these figures show significant demarcation between mild-to-moderate and severe hemiparesis, with AM showing more clarity among the two classes and OM showing more overlap. These figures indicate that the proposed features can be used to design classifier models for identifying hemiparetic severity using only short-length spontaneous motion data.

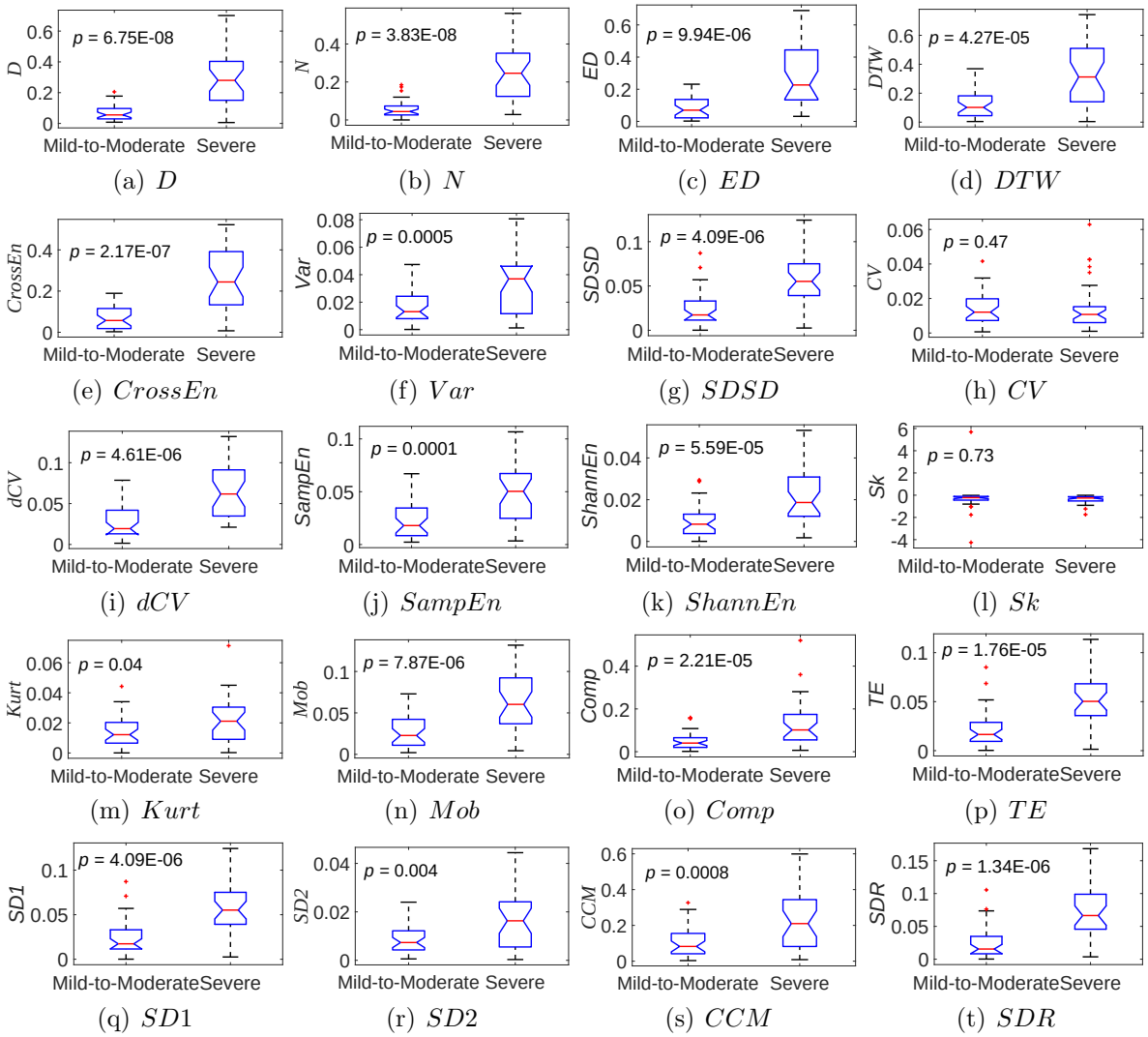

Figure 4: Distribution of features derived from velocity profiles of movement elements in AM shown using box plots across two classes of hemiparetic severity. p-value represents the statistical significance in Kruskal Wallis test.

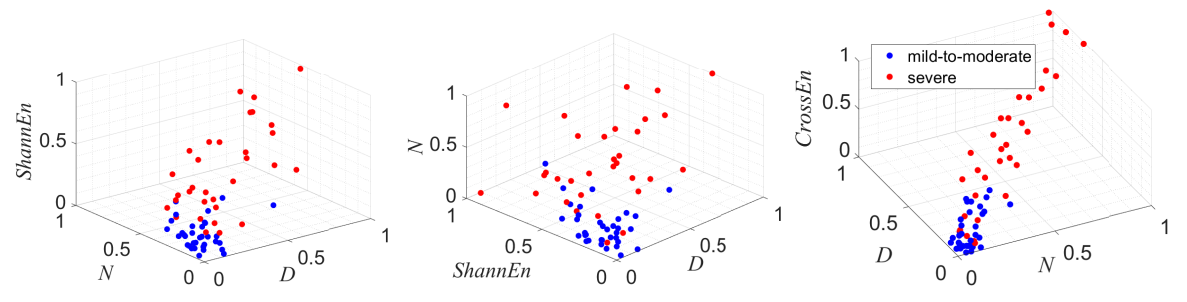

Figure 5: 3D scatter plots of top three features based on AUC values (as observed in Table 3), from each type of movement. The plots show clear distinction between mild-to-moderate and severe hemiparesis.

Table 3: Evaluation of extracted features through statistical tests and ROC analysis

Feature	AUC			Feature	AUC		
	HM	OM	AM		HM	OM	AM
D	0.86^{+}	0.88^{+}	0.88^{+}	$ShannEn$	0.83^{+}	0.85^{+}	0.80^{+}
N	0.84^{+}	0.82^{+}	0.89^{+}	Sk	0.55	0.56	0.52
ED	0.80^{+}	0.75^{+}	0.81^{+}	$Kurt$	0.73^{*}	0.61	0.64
DTW	0.80^{+}	0.74^{+}	0.79^{+}	Mob	0.78^{+}	0.72^{+}	0.80^{+}
$CrossEn$	0.81^{+}	0.77^{+}	0.89^{+}	$Comp$	0.75^{+}	0.76^{*}	0.82^{+}
Var	0.73^{*}	0.76^{+}	0.75^{+}	TE	0.74^{+}	0.77^{+}	0.81^{+}
$SDSD$	0.75^{+}	0.76^{+}	0.83^{+}	$SD1$	0.75^{+}	0.76^{+}	0.83^{+}
CV	0.52	0.53	0.55	$SD2$	0.77^{+}	0.76^{+}	0.75^{*}
dCV	0.77^{+}	0.66	0.83^{+}	CCM	0.69^{*}	0.73^{*}	0.74^{+}
$SampEn$	0.69^{*}	0.72^{*}	0.77^{+}	SDR	0.69^{*}	0.80^{+}	0.84^{+}

* and $^{+}$ imply statistical significance with $p < 0.01$ and $p < 0.001$ respectively

4.3. Classification of Hemiparesis

The results of classification with MRMR feature selection, using different types of SVM kernels across 10-folds of cross-validation are presented in Table 4. We find that a Gaussian kernel leads to the highest mean accuracy of 0.85 in a 10-fold classification. It is to be noted that each classifier results in high sensitivities (> 0.80) in identifying both mild-to-moderate and severe hemiparesis, leading to decent F-scores. Fig. 6 illustrates the feature selection process and classification decision boundaries respectively, produced by the Gaussian SVM in a randomly selected fold during cross-validation. It can be observed from Fig. 6(a) that the top features belong to HM and AM. Fig. 6(b) shows a clear separation of mild-to-moderate and severe hemiparesis by the SVM decision boundary with minor miss-classifications. The features that were always selected among the top 20 across all cross-validation folds included N, D, $ShannEn$, Mob, ED, $SDSD$ and $SD1$ of HM and N, D, $ShannEn$, $CrossEn$, TE, SDR and dCV of AM.

Table 4: Classification performance of proposed features using SVM through 10-fold cross-validation showing mean ± standard deviation of the metrics across all folds

SVM Kernel	Accuracy	Sensitivity (Mild-to-moderate)	Sensitivity (Severe)	F-score
Linear	0.80 ± 0.16	0.86 ± 0.20	0.82 ± 0.18	0.73 ± 0.12
Gaussian	0.85 ± 0.14	0.84 ± 0.18	0.89 ± 0.14	0.82 ± 0.20
Quadratic	0.80 ± 0.14	0.83 ± 0.19	0.82 ± 0.21	0.70 ± 0.28
Cubic	0.79 ± 0.17	0.80 ± 0.20	0.81 ± 0.24	0.69 ± 0.28

5. Discussion

Literature provides evidence of the existence of basic units of movement that subjects perform to completion after the initiation of any motion [39]. This has been recently

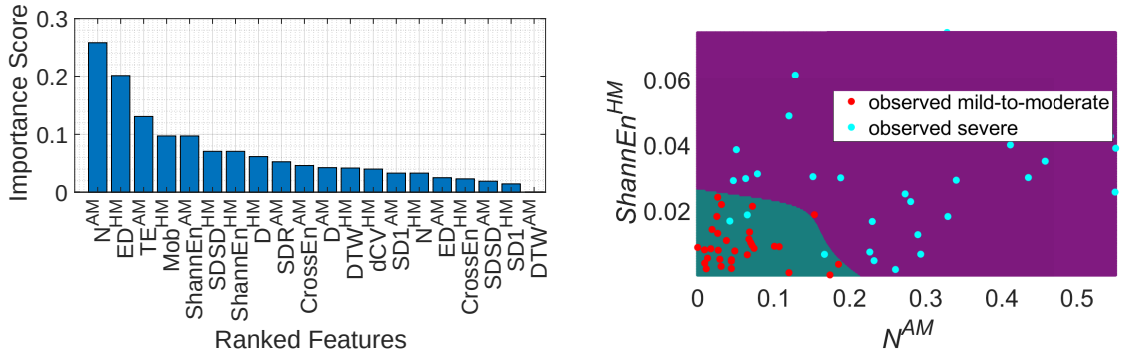

(a) (b)

Figure 6: Classification of hemiparesis using selected features in a randomly selected cross-validation fold showing (a) feature importance scores obtained from MRMR analysis (only top features with scores above zero are illustrated) and (b) decision boundaries with a Gaussian kernel in a 2D plane (with top two features only, due to visual representation limitations) separating mild-to-moderate and severe hemiparesis.

investigated to show that complex upper limb motion can indeed be decomposed into basic units of point-to-point motion resembling simple reaching tasks [25]. In this work, we have used wearable sensor data to show that upper limb motion in stroke survivors also follow this principle. By decomposing completely spontaneous upper limb motion into component movement elements, we have computed novel features to describe the quality of such motion. Further, we have shown that these features bear correlation with the degree of hemiparesis in acute stroke. A major difference and improvement of this work over recent literature is the study of the relative characteristics of the movement elements between two hands, compared to studying the absolute motion of the affected hand [20] or using data acquired from healthy *control* subjects to identify homogeneous movement elements [19].

5.1. Interpretation of the Characteristics of Movement Elements

Smoothness is a characteristic of co-ordinated human movements [40]. Early works have shown that infants perform simple hand motion by combining movement elements that become smoother over periods of learning [41,42]. Humans, without conscious input, can plan motion during complex tasks by focusing on small task segments. During simple reaching tasks, the human central nervous system performs an optimization process aimed at minimizing jerk and task duration that produces smooth velocity profiles [19, 24]. In this work, we showed that while spontaneous motion in the hemiparetic hand of stroke survivors do follow the minimum-jerk principle, the movement elements in the normal hand are significantly smoother than the hemiparetic hand. We quantified this difference by extracting various features from the individual movement elements to study the quality of upper limb motion in stroke survivors. The features that were extracted comprised (i) the number and duration of movement elements, (ii) their similarity or deviation from the average movement element of the set, computed using

standard distance measures and (iii) various statistical measures of the velocity time series representing the smoothness of individual movement elements. All features were computed as relative measures between two hands and the difference was found to be significantly higher in severe hemiparesis than in mild-to-moderate hemiparesis. Our experiments show that the movement elements in stroke survivors increase in number with smaller duration with increasing hemiparetic severity. The number (and density) of movement elements relates to irregular and jerky motion in the hemiparetic hand resulting in a large number of zero crossings [19, 20]. The characteristics of duration follows [19], showing that the average time length of movement elements in stroke impaired subjects significantly reduces with hemiparetic severity. This actually relates to (4), where the duration of the point-to-point reaching movement increases with distance traversed. It has been observed that upper limb motor impairment in stroke is often associated with a limited range of motion [20, 43], thereby reducing D and in turn, t_f for each movement element.

From Table 3, we can make some observations on the goodness of the other features in identifying hemiparesis as well. The distance features are particularly useful, as these, capture the deviation of the elements from the mean, and therefore are distinctly higher in the hemiparetic hand. The features Var, dCV, Mob, $Comp$ and TE are well known quantifiers of randomness and variability in a time series, predominantly used in heart rate variability analysis [36, 44]. Therefore these features perform well in quantifying the jerky movements in the present context as well. Among the entropy features, $ShannEn$ performs better than $SampEn$. This is because, $SampEn$ is concerned with repetitive patterns within the time series, which may or may not quantify the jerky nature well [33]. $ShannEn$, on the other hand, quantifying the overall uncertainty in a time series, captures the difference between smooth and irregular patterns better. Among the Poincaré features, we observe that $SD1$ and SDR (which is composed of $SD1$) are more discriminative that the others. This is primarily because $SD1$ encodes short-term variability, unlike $SD2$ (which represents long-term variability) in a time series [31]. In the present context, the long-term variability of all data are similar (*e.g.*, the shape resembles a bell-shaped or near bell-shaped curve for HM), whereas, the short-term variability given by the jerkiness or smoothness is higher in hemiparesis.

Our results corroborate with very early clinical findings reported in [45] and later in [40]. These works used robot assisted manipulative devices to measure smoothness of motion in stroke survivors. Using kinematic analysis it was shown that individual movement speed profiles during continuous hand motion in unloaded tasks, was invariant across patients with different types of stroke aetiology and was similar to the shape of primitive movement elements following the minimum jerk principle [45]. The overall shape of speed profiles were unaffected by the peak speed and they appeared jerky. Further, it was found that the movement elements seem to grow smoother with time as the patients recovered [40]. It is to be noted that, as in [20], the homogeneous movement elements in the present context do not particularly refer to healthy movements. It is interesting that the homogeneous movements in the hemiparetic hand are jerky

compared to the normal hand and the amount of this disparity increases with the severity of hemiparesis. Further, the differentiation between the denser homogeneous set and sparser outlier set can be useful in determining hemiparetic severity. As observed from Fig. 6(a), the top features selected across all types of elements in distinguishing the two classes of hemiparesis belong particularly to the homogeneous set, other than all movement elements.

5.2. Effect of Noise on Hemiparesis Identification

An interesting angle in this work is to study the goodness of the proposed velocity profile based features in identifying the severity of hemiparesis. Existing literature in this direction use different forms of descriptors that ultimately measure the amount of *activity* of the affected hand. In our recent works [5, 16, 17], we have described such activity based measures quantifying the relative motion between two hands that correlated well with NIHSS scores in acute stroke. However, being based on activity only, these measures are extremely susceptible to the effect of additive noise. Additive high amplitude noise of any nature would increase the energy content and activity of the affected hand, despite not being actual activity performed by the patient, during spontaneous data acquisition. This is very common in a hospital environment, where external touch by a nurse or other high amplitude artefacts can contribute to the increase in the activity levels of the affected hand. An important consideration in this respect is that the features proposed in this work measure the quality of motion by analyzing the density, duration and smoothness of the velocity profiles. These are not affected by the amplitude of the acceleration signal. Fig. 7 presents the effect of adding external noise in the affected hand on the proposed features in identifying mild-to-moderate and severe hemiparesis. The raw accelerometer data of affected hand is segmented into non-overlapping windows of 5 seconds duration and in some of these windows, high amplitude (upto the maximum amplitude of the signal) noise is added at random locations. The amount of noise affected windows indicates the percentage of added noise. We can observe from Figs. 7(a) and 7(b) that addition of noise do not affect the value of AUC. However, in Fig.7(c), which illustrates the performance of *activity coherence* features proposed in our earlier work [5], the effect of noise is extremely significant. Here, the AUC deteriorates by 20% even upon the addition of 5% noise to the raw data. Therefore, the proposed method is particularly useful in identifying hemiparetic severity from noisy data by eliminating motion artefacts.

It is to be noted that we have only identified two levels of hemiparetic severity using this approach, and there remains a scope of further improving clinical granularity in identifying sub-classes of hemiparesis. However, the motor component of NIHSS comprise only a part of stroke severity assessment. Medical personnel are mostly interested in getting a broad idea of improvement or deterioration of hemiparetic severity (from mild-to-moderate to severe hemiparesis) indicated by several NIHSS factors [46,47]. Additionally, clinical granularity in defining further levels of hemiparesis

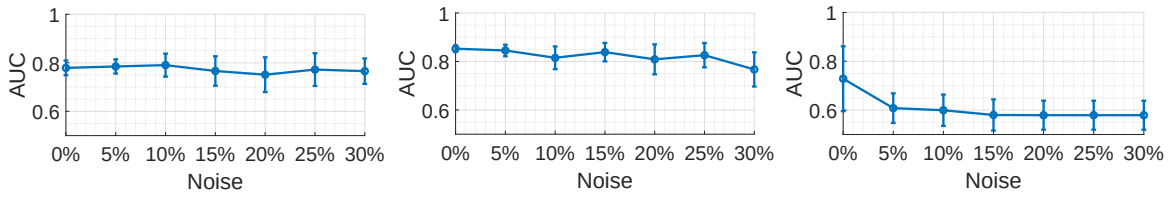

(a) Features from HM (b) Features from AM (c) Activity based features [5]

Figure 7: Performance comparison showing the effect of adding noise to raw accelerometer data in identifying hemiparetic severity. The mean and standard deviation of AUC of the top ten features are considered in (a) and (b), and all features found statistically significant in [5] is considered in (c).

is highly subjective and suffers from inter-rater variability [5, 48]. Therefore, the proposed model based only on spontaneous motion and two sensors, can be sufficiently effective in providing a general idea of hemiparesis progression in the clinical scenario.

6. Conclusion

In this study, we have shown that completely spontaneous upper limb motion in acute stroke patients can be decomposed into component elements that resemble 1D point-to-point movements. These movement elements show different characteristics for the normal and the hemiparetic hands, in terms of density, duration and smoothness. The disparity of such measures between the two hands can be used to identify hemiparesis and further classify the severity of hemiparesis with references to the clinical gold standard NIHSS scores. The proposed measures bear physiological significance with clinical results reported in the existing literature. This work shows the feasibility of analyzing the quality of upper limb motion planned by the central nervous system using wearable sensors, instead of simply quantifying the amount of activity to identify hemiparesis in stroke survivors. The work is particularly significant in the clinical scenario as it involves completely spontaneous activities acquired using only two wrist-worn sensors, thereby avoiding any physical burden or obtrusion for patients, while being robust towards additive noise in the acquired data. Future scopes of this work include improvement of clinical sensitivity in identifying sub-classes of hemiparesis for continuous monitoring in a hospital or remote monitoring at home.

Acknowledgement

This work is supported by the Australian Research Council (ARC) Discovery Project (DP190101248) grant.

References

[1] B. Norrving and B. Kissela, "The global burden of stroke and need for a continuum of care," *Neurology*, vol. 80, no. 3, supplement 2, pp. S5–S12, 2013.

[2] M. P. Lindsay, B. Norrving, R. L. Sacco, M. Brainin, W. Hacke, S. Martins, J. Pandian, and V. Feigin, "World stroke organization (wso): global stroke fact sheet 2019," 2019.

[3] P. Raghavan, "Upper limb motor impairment after stroke," *Physical Medicine and Rehabilitation Clinics*, vol. 26, no. 4, pp. 599–610, 2015.

[4] A. Davalos, D. Toni, F. Iweins, E. Lesaffre, S. Bastianello, and J. Castillo, "Neurological deterioration in acute ischemic stroke: potential predictors and associated factors in the european cooperative acute stroke study (ecass) I," *Stroke*, vol. 30, no. 12, pp. 2631–2636, 1999.

[5] S. Datta, C. K. Karmakar, A. S. Rao, B. Yan, and M. Palaniswami, "Automated scoring of hemiparesis in acute stroke from measures of upper limb co-ordination using wearable accelerometry," *IEEE Transactions on Neural Systems and Rehabilitation Engineering*, vol. 28, no. 4, pp. 805–816, 2020.

[6] J. Gubbi, A. S. Rao, K. Fang, B. Yan, and M. Palaniswami, "Motor recovery monitoring using acceleration measurements in post acute stroke patients," *Biomedical engineering online*, vol. 12, no. 1, p. 33, 2013.

[7] C. Weimar, T. Mieck, J. Buchthal, C. E. Ehrenfeld, E. Schmid, and H.-C. Diener, "Neurologic worsening during the acute phase of ischemic stroke," *Archives of neurology*, vol. 62, no. 3, pp. 393–397, 2005.

[8] C. Le Heron, K. Fang, J. Gubbi, L. Churilov, M. Palaniswami, S. Davis, and B. Yan, "Wireless accelerometry is feasible in acute monitoring of upper limb motor recovery after ischemic stroke," *Cerebrovascular Diseases*, vol. 37, no. 5, pp. 336–341, 2014.

[9] C. E. Lang, J. M. Wagner, D. F. Edwards, and A. W. Dromerick, "Upper extremity use in people with hemiparesis in the first few weeks after stroke," *Journal of Neurologic Physical Therapy*, vol. 31, no. 2, pp. 56–63, 2007.

[10] T. Hester, R. Hughes, D. M. Sherrill, B. Knorr, M. Akay, J. Stein, and P. Bonato, "Using wearable sensors to measure motor abilities following stroke," in *International Workshop on Wearable and Implantable Body Sensor Networks (BSN)*, 2006, pp. 4 pp.–8.

[11] S. Patel, R. Hughes, T. Hester, J. Stein, M. Akay, J. G. Dy, and P. Bonato, "A novel approach to monitor rehabilitation outcomes in stroke survivors using wearable technology," *Proceedings of the IEEE*, vol. 98, no. 3, pp. 450–461, 2010.

[12] S. Patel, R. Hughes, T. Hester, J. Stein, M. Akay, J. Dy, and P. Bonato, "Tracking motor recovery in stroke survivors undergoing rehabilitation using wearable technology," in *International Conference of the IEEE Engineering in Medicine and Biology Society (EMBC)*, 2010, pp. 6858–6861.

[13] S. Del Din, S. Patel, C. Cobelli, and P. Bonato, "Estimating fugl-meyer clinical scores in stroke survivors using wearable sensors," in *International Conference of the IEEE Engineering in Medicine and Biology Society (EMBC)*, 2011, pp. 5839–5842.

[14] H.-T. Li, J.-J. Huang, C.-W. Pan, H.-I. Chi, and M.-C. Pan, "Inertial sensing based assessment methods to quantify the effectiveness of post-stroke rehabilitation," *Sensors*, vol. 15, no. 7, pp. 16 196–16 209, 2015.

[15] D. Kumar, J. Gubbi, B. Yan, and M. Palaniswami, "Motor recovery monitoring in post acute stroke patients using wireless accelerometer and cross-correlation," in *International Conference of the IEEE Engineering in Medicine and Biology Society (EMBC)*, 2013, pp. 6703–6706.

[16] S. Datta, C. K. Karmakar, B. Yan, and M. Palaniswami, "Poincare descriptors for identifying hemiparesis in acute stroke using wearable accelerometry," in *International Conference of the IEEE Engineering in Medicine and Biology Society (EMBC)*, 2020.

[17] ——, "Analyzing distance measures for upper limb activity measurement in hemiparetic stroke patients," in *International Conference of the IEEE Engineering in Medicine and Biology Society*

(EMBC), 2020.

[18] K. S. Hayward, J. J. Eng, L. A. Boyd, B. Lakhani, J. Bernhardt, and C. E. Lang, "Exploring the role of accelerometers in the measurement of real world upper-limb use after stroke." *Brain Impairment*, vol. 17, no. 1, 2016.

[19] S. I. Lee, H.-T. Jung, J. Park, J. Jeong, T. Ryu, Y. Kim, V. S. Dos Santos, J. G. V. Miranda, and J.-F. Daneault, "Towards the ambulatory assessment of movement quality in stroke survivors using a wrist-worn inertial sensor," in *International Conference of the IEEE Engineering in Medicine and Biology Society (EMBC)*, 2018, pp. 2825–2828.

[20] B. Oubre, J.-F. Daneault, H.-T. Jung, K. Whritenour, J. G. V. Miranda, J. Park, T. Ryu, Y. Kim, and S. I. Lee, "Estimating upper-limb impairment level in stroke survivors using wearable inertial sensors and a minimally-burdensome motor task," *IEEE Transactions on Neural Systems and Rehabilitation Engineering*, vol. 28, no. 3, pp. 601–611, 2020.

[21] N. Hogan, "An organizing principle for a class of voluntary movements," *Journal of Neuroscience*, vol. 4, no. 11, pp. 2745–2754, 1984.

[22] T. Flash and N. Hogan, "The coordination of arm movements: an experimentally confirmed mathematical model," *Journal of Neuroscience*, vol. 5, no. 7, pp. 1688–1703, 1985.

[23] S. Datta, C. Karmakar, B. Yan, and M. swami Palaniswami, "Novel measures of similarity and asymmetry in upper limb activities for identifying hemiparetic severity in stroke survivors," *IEEE Journal of Biomedical and Health Informatics*, 2020.

[24] B. Hoff, "A model of duration in normal and perturbed reaching movement," *Biological Cybernetics*, vol. 71, no. 6, pp. 481–488, 1994.

[25] J. G. V. Miranda, J.-F. Daneault, G. Vergara-Diaz, A. P. Quixadá, M. de Lemos Fonseca, J. P. B. C. Vieira, V. S. dos Santos, T. C. da Figueiredo, E. B. Pinto, N. Peña *et al.*, "Complex upper-limb movements are generated by combining motor primitives that scale with the movement size," *Scientific reports*, vol. 8, no. 1, pp. 1–11, 2018.

[26] J. Bamford, P. Sandercock, M. Dennis, C. Warlow, and J. Burn, "Classification and natural history of clinically identifiable subtypes of cerebral infarction," *The Lancet*, vol. 337, no. 8756, pp. 1521–1526, 1991.

[27] M. J. Mathie, A. C. Coster, N. H. Lovell, and B. G. Celler, "Accelerometry: providing an integrated, practical method for long-term, ambulatory monitoring of human movement," *Physiological measurement*, vol. 25, no. 2, p. R1, 2004.

[28] S. Datta, J. C. Bezdek, and M. Palaniswami, "Experiments with dissimilarity measures for clustering waveform data from wearable sensors," in *IEEE Symposium Series on Computational Intelligence (SSCI)*, 2019.

[29] J. Paparrizos and L. Gravano, "k-shape: Efficient and accurate clustering of time series," in *Proceedings of the ACM SIGMOD International Conference on Management of Data*, 2015, pp. 1855–1870.

[30] R. K. Udhayakumar, C. Karmakar, and M. Palaniswami, "Cross entropy profiling to test pattern synchrony in short-term signals," in *2019 41st Annual International Conference of the IEEE Engineering in Medicine and Biology Society (EMBC)*, 2019, pp. 737–740.

[31] M. Brennan, M. Palaniswami, and P. Kamen, "Do existing measures of poincare plot geometry reflect nonlinear features of heart rate variability?" *IEEE Transactions on Biomedical Engineering*, vol. 48, no. 11, pp. 1342–1347, 2001.

[32] S. Kusmakar, C. Karmakar, B. Yan, R. Muthuganapathy, P. Kwan, T. J. O'Brien, and M. S. Palaniswami, "Novel features for capturing temporal variations of rhythmic limb movement to distinguish convulsive epileptic and psychogenic nonepileptic seizures," *Epilepsia*, vol. 60, no. 1, pp. 165–174, 2019.

[33] R. K. Udhayakumar, C. Karmakar, and M. Palaniswami, "Understanding irregularity characteristics of short-term hrv signals using sample entropy profile," *IEEE Transactions on Biomedical Engineering*, vol. 65, no. 11, pp. 2569–2579, 2018.

[34] D. Kugiumtzis and A. Tsimpiris, "Measures of analysis of time series (mats): a matlab toolkit for

computation of multiple measures on time series data bases," *arXiv preprint arXiv:1002.1940*, 2010.

[35] C. K. Karmakar, A. H. Khandoker, J. Gubbi, and M. Palaniswami, "Complex correlation measure: a novel descriptor for poincaré plot," *Biomedical engineering online*, vol. 8, no. 1, p. 17, 2009.

[36] M. A. Motin, C. Kamakar, P. Marimuthu, and T. Penzel, "Photoplethysmographic-based automated sleep–wake classification using a support vector machine," *Physiological Measurement*, vol. 41, no. 7, p. 075013, 2020.

[37] C. Ding and H. Peng, "Minimum redundancy feature selection from microarray gene expression data," *Journal of bioinformatics and computational biology*, vol. 3, no. 02, pp. 185–205, 2005.

[38] *MATLAB version 9.7.0.1296695 (R2019b)*, The Mathworks, Inc., Natick, Massachusetts, 2019.

[39] R. Sosnik, E. Chaim, and T. Flash, "Stopping is not an option: the evolution of unstoppable motion elements (primitives)," *Journal of neurophysiology*, vol. 114, no. 2, pp. 846–856, 2015.

[40] B. Rohrer, S. Fasoli, H. I. Krebs, R. Hughes, B. Volpe, W. R. Frontera, J. Stein, and N. Hogan, "Movement smoothness changes during stroke recovery," *Journal of Neuroscience*, vol. 22, no. 18, pp. 8297–8304, 2002.

[41] N. E. Berthier, "Learning to reach: a mathematical model." *Developmental psychology*, vol. 32, no. 5, p. 811, 1996.

[42] D. Corbetta and E. Thelen, "The developmental origins of bimanual coordination: a dynamic perspective." *Journal of Experimental Psychology: Human Perception and Performance*, vol. 22, no. 2, p. 502, 1996.

[43] D. G. Kamper, A. N. McKenna-Cole, L. E. Kahn, and D. J. Reinkensmeyer, "Alterations in reaching after stroke and their relation to movement direction and impairment severity," *Archives of physical medicine and rehabilitation*, vol. 83, no. 5, pp. 702–707, 2002.

[44] A. Mukherjee, A. D. Choudhury, S. Datta, C. Puri, R. Banerjee, R. Singh, A. Ukil, S. Bandyopadhyay, A. Pal, and S. Khandelwal, "Detection of atrial fibrillation and other abnormal rhythms from ecg using a multi-layer classifier architecture," *Physiological measurement*, vol. 40, no. 5, 2019.

[45] H. I. Krebs, M. L. Aisen, B. T. Volpe, and N. Hogan, "Quantization of continuous arm movements in humans with brain injury," *Proceedings of the National Academy of Sciences*, vol. 96, no. 8, pp. 4645–4649, 1999.

[46] F. S. Vahidy, W. J. Hicks, I. Acosta, H. Hallevi, H. Peng, R. Pandurengan, N. R. Gonzales, A. D. Barreto, S. Martin-Schild, T.-C. Wu *et al.*, "Neurofluctuation in patients with subcortical ischemic stroke," *Neurology*, vol. 83, no. 5, pp. 398–405, 2014.

[47] O. Ozdemir, V. Beletsky, R. Chan, and V. Hachinski, "Thrombolysis in patients with marked clinical fluctuations in neurologic status due to cerebral ischemia," *Archives of neurology*, vol. 65, no. 8, pp. 1041–1043, 2008.

[48] C. D. Bushnell, D. C. Johnston, and L. B. Goldstein, "Retrospective assessment of initial stroke severity: comparison of the nih stroke scale and the canadian neurological scale," *Stroke*, vol. 32, no. 3, pp. 656–660, 2001.